Published in final edited form as:
Cell Host Microbe. 2011 January 20; 9(1): 46–57. doi:10.1016/j.chom.2010.12.005.

Compensatory Changes in the Cytoplasmic Tail of gp41 Confer Resistance to Tetherin/BST-2 in a Pathogenic Nef-deleted SIV

Ruth Serra-Moreno[1], **Bin Jia**[1], **Matthew Breed**[2], **Xavier Alvarez**[2], and **David T. Evans**[1,*]

[1]Department of Microbiology and Molecular Genetics, Harvard Medical School, New England Primate Research Center, Southborough, MA 01772-9102

[2]Division of Comparative Pathology, Tulane National Primate Research Center, Covington, LA 70433-8915

SUMMARY

Tetherin (BST-2 or CD317) is an interferon-inducible transmembrane protein that inhibits virus release from infected cells. Whereas HIV-1 Vpu and HIV-2 Env counteract human tetherin, most SIVs use Nef to antagonize the tetherin proteins of their non-human primate hosts. Here we show that compensatory changes in the cytoplasmic domain of SIV gp41, acquired by a *nef*-deleted virus that regained a pathogenic phenotype in infected rhesus macaques, restore resistance to tetherin. These changes facilitate virus release in the presence of rhesus tetherin, but not human tetherin, and enhance virus replication in interferon-treated primary lymphocytes. The substitutions in gp41 result in a selective physical association with rhesus tetherin, and the internalization and sequestration of rhesus tetherin by a mechanism that depends on a conserved endocytosis motif in gp41. These results are consistent with HIV-2 Env antagonism of human tetherin, and suggest that the ability to oppose tetherin is important for lentiviral pathogenesis.

INTRODUCTION

Mammalian cells have evolved a number of restriction factors to interfere with different stages of virus replication (Wolf and Goff, 2008). One such factor, tetherin (BST-2, CD317 or HM1.24), impairs the detachment of enveloped viruses from infected cells (Kaletsky et al., 2009; Neil et al., 2008; Neil et al., 2007; Van Damme et al., 2008). Tetherin is a type II integral membrane protein with a topology that allows both ends of the protein to be anchored in lipid membranes (Kupzig et al., 2003). It has an N-terminal cytoplasmic domain followed by a transmembrane domain, an extracellular coiled-coil domain and a C-terminal glycosyl-phosphatidylinositol (GPI) anchor (Kupzig et al., 2003; Rollason et al., 2007). Under conditions of interferon-induction, tetherin is upregulated and becomes incorporated into virus particles as they attempt to bud from infected cells (Fitzpatrick et al., 2010; Hammonds et al., 2010; Perez-Caballero et al., 2009). Recent evidence suggests that tetherin

*Corresponding author: David T. Evans, Ph.D., Department of Microbiology and Molecular Genetics, Harvard Medical School, New England Primate Research Center, One Pine Hill Drive, Southborough, Massachusetts 01772-9102, Phone: (508) 786-8025, Fax: (508) 786-3317. david_evans@hms.harvard.edu.

The authors have no conflicting financial interests.

Author contributions: DTE and RSM designed the experiments. RSM, BJ, MB and XA performed the experiments and analyzed the data. RSM and DTE wrote the manuscript.

forms a parallel homodimer that physically bridges nascent virus particles to infected cells (Perez-Caballero et al., 2009). Captured virions are then internalized and routed to endosomal compartments for degradation by a mechanism that involves interactions of the cytoplasmic domain of tetherin with the endocytosis machinery of the cell and with BCA2 (breast cancer-associated gene 2) (Gottlinger, 2008; Miyakawa et al., 2009; Perez-Caballero et al., 2009).

Tetherin has a broad spectrum of antiviral activity against diverse families of enveloped viruses including retroviruses, filoviruses, herpesviruses and arenaviruses (Jouvenet et al., 2009; Mansouri et al., 2009; Sakuma et al., 2009). Many of these viruses have in turn evolved specific countermeasures to tetherin (Jia et al., 2009; Kaletsky et al., 2009; LeTortorec and Neil, 2009; Neil et al., 2008; Van Damme et al., 2008; Zhang et al., 2009). Among the primate lentiviruses, three different viral gene products are known to antagonize tetherin. Whereas HIV-1 Vpu and HIV-2 Env antagonize human tetherin (LeTortorec and Neil, 2009; Neil et al., 2008; Van Damme et al., 2008), the majority of SIVs use Nef to counteract the tetherin proteins of their simian hosts (Jia et al., 2009; Sauter et al., 2009; Zhang et al., 2009).

A role for Nef in counteracting restriction by tetherin may help to explain the attenuated phenotype of *nef*-deleted SIV in rhesus macaques (Kestler et al., 1991). In SIV Δ*nef*-infected macaques, peak viral loads are typically two to three logs lower than peak viral loads in wild-type SIV infected animals, and chronic phase viral loads are often contained below the limit of detection (Kestler et al., 1991). Nevertheless, a certain percentage of animals infected with *nef*-deleted SIV develop moderate viral loads and progress to AIDS after prolonged periods of persistent infection (Alexander et al., 2003; Baba et al., 1995; Baba et al., 1999; Wyand et al., 1997). This increase in replicative capacity reflects the accumulation of genetic changes that restore a pathogenic phenotype, since *nef*-deleted viruses isolated from animals that progress to disease also cause disease in newly infected animals (Alexander et al., 2003).

Here we show that a pathogenic clone of SIV Δ*nef*, containing nucleotide changes acquired after serial passage of *nef*-deleted SIV in rhesus macaques (Alexander et al., 2003), is resistant to restriction by rhesus tetherin. This resistance mapped to specific amino acid substitutions in the cytoplasmic domain of gp41 that confer resistance to rhesus tetherin, but not to human tetherin. These compensatory changes result in the selective co-immunopreciptation of Env with rhesus tetherin, facilitate virus replication in interferon-treated lymphocytes, and promote the internalization and sequestration of tetherin in infected primary lymphocytes. These results are entirely consistent with a role for the HIV-2 envelope glycoprotein in counteracting human tetherin (Abada et al., 2005; Bour et al., 1996; LeTortorec and Neil, 2009), and suggest that the ability to overcome restriction by tetherin is particularly important for lentiviral pathogenesis.

RESULTS

Compensatory genetic changes acquired by a pathogenic, *nef*-deleted strain of SIV confer resistance to rhesus tetherin

Analysis of the nucleotide sequence changes acquired by pathogenic isolates of *nef*-deleted SIV after serial passage in rhesus macaques revealed the accumulation of changes in three regions of the viral genome (Alexander et al., 2003). These included a cluster of non-synonymous changes in *env* coding for amino acid substitutions in the gp41 cytoplasmic domain, an expanded deletion of *nef* sequences overlapping with U3, and a duplication of the NF-κB binding site (Alexander et al., 2003). By engineering these changes back into $SIV_{mac}239$ Δ*nef*, Alexander *et al.* demonstrated that the changes in the gp41 tail (termed

ITM for "improved transmembrane"), and an additional 278 bp deletion in U3 (ΔU3), were sufficient for pathogenesis (Alexander et al., 2003). Since the envelope glycoproteins of certain HIV-2 isolates can counteract tetherin (Abada et al., 2005; Hauser et al. 2010; Jia et al., 2009; LeTortorec and Neil, 2009), we hypothesized that these compensatory changes, particularly the ITM changes in gp41, might provide resistance to tetherin.

To test this hypothesis, we compared virus release for SIV ITMΔ*nef*ΔU3, which we refer to hereafter as SIV Δ*nefP*, to virus release for SIV Δ*nef* and wild-type SIV at increasing expression levels of human and rhesus tetherin. Since tetherin is polymorphic in the rhesus macaque (McNatt et al., 2009), we tested three different alleles; rBST-2.1, rBST-2.2 and rBST-2.8 (Figure S1). rBST-2.1 and rBST-2.2 represent common alleles, whereas rBST-2.8 was cloned from cryopreserved PBMCs of the animal from which the compensatory changes in SIV Δ*nefP* were first isolated. Wild-type SIV, SIV Δ*nef* and SIV Δ*nefP* all exhibited similar susceptibility to restriction by human tetherin (Figure 1A). However, these viruses differed in their susceptibility to rhesus tetherin. Whereas SIV Δ*nef* remained susceptible to restriction, wild-type SIV and SIV Δ*nefP* were resistant to all three alleles. In the presence of rBST-2.1 and rBST-2.8, the release of SIV Δ*nefP* was similar to wild-type SIV (Figures 1B and 1D). However, in the presence of rBST-2.2, the release of SIV Δ*nefP* was higher than SIV Δ*nef*, but did not reach the same levels as wild-type virus (Figure 1C). This difference may reflect the incomplete adaptation of SIV Δ*nefP* to rBST-2.2, since the predicted amino acid sequence of this allele differs from both rBST-2.1 and rBST-2.8 by three residues ($D_{14}G$, $V_{29}I$ and $P_{159}S$) (Figure S1). Nevertheless, for each of the rBST-2 alleles that were tested, virus release for SIV Δ*nefP* was consistently higher than for SIV Δ*nef*, indicating that the compensatory changes acquired by SIV Δ*nefP* afford broad resistance to different alleles of rhesus tetherin.

The resistance of SIV Δ*nefP* to restriction by rhesus tetherin was corroborated by western blot analysis. Consistent with previous observations (Jia et al., 2009), cell-associated Env and p55 Gag levels diminished under conditions of tetherin overexpression for each of the three viruses. However, at increasing expression levels of rhesus tetherin (rBST-2.1), the accumulation of p27 in the cell culture supernatant was consistently greater for SIV Δ*nefP* than for SIV Δ*nef* (Figure 1E). Moreover, similar to wild-type SIV, virion-associated p27 remained detectable for SIV Δ*nefP*, even at the highest expression levels of rhesus tetherin (Figure 1E). Hence, these results further indicate that the compensatory changes in SIV Δ*nefP* afford resistance to the inhibitory effects of rhesus tetherin on virion release.

The compensatory changes in SIV Δ*nefP* facilitate virus replication under conditions of interferon-induced upregulation of tetherin

To determine if the compensatory changes in SIV Δ*nefP* enhance virus replication under more physiological conditions of tetherin expression, virus replication was assessed in interferon-treated rhesus macaque lymphocytes. Activated PBMCs from three different animals were infected with wild-type SIV, SIV Δ*nef* and SIV Δ*nefP*. On day two post-infection, the cultures were divided and maintained in medium with or without IFNα. The upregulation of tetherin on $CD4^+$ lymphocytes was verified by flow cytometry (Figure 2A), and virus replication was monitored by the accumulation of SIV p27 in the cell culture supernatant (Figures 2B–2G). In the absence of IFNα, each of the viruses replicated with similar kinetics (Figures 2B, 2D and 2F). Treatment with IFNα suppressed the replication of all three viruses. However, whereas SIV Δ*nef* was severely inhibited, SIV Δ*nefP* and wild-type SIV were more resistant and replicated to similar levels (Figures 2C, 2E, and 2G). Hence, the changes acquired by SIV Δ*nefP* facilitate virus replication under conditions of interferon-induced upregulation of tetherin in primary rhesus macaque lymphocytes.

Amino acid substitutions in the cytoplasmic tail of gp41 afford resistance to rhesus tetherin

To identify the sequence changes in SIV Δ*nefP* that confer resistance to rhesus tetherin, the ITM and ΔU3 mutations were introduced separately into SIV Δ*nef* (Figure 3A), and these recombinant proviruses were tested for their susceptibility to restriction by rhesus tetherin (Figure 3B). While the U3 deletion resulted in a marginal increase in virus release relative to SIV Δ*nef* (< 2-fold), the ITM changes restored virus release to the same level as SIV Δ*nefP* (Figure 3B). The envelope glycoprotein of SIV Δ*nefP*, EnvITM, was therefore tested for the ability to rescue particle release for an *env*- and *nef*-deleted strain of SIV in the presence of rhesus tetherin. EnvITM, but not wild-type Env, restored the release of SIV Δ*env*Δ*nef* to a level approaching the extent of virus release afforded by Nef, as measured by p27 antigen-capture ELISA (Figure 3C) and by western blot analysis (Figure 3D). Thus, the envelope glycoprotein expressed by SIV Δ*nefP* antagonizes restriction by rhesus tetherin.

Additional sequence changes were identified in the remainder of the *nef* open-reading frame, not reported in the initial description of SIV Δ*nefP* (Alexander et al., 2003), which encode a unique 94 amino acid polypeptide we refer to as pseudo-Nef (ψNef) (Figure S2A). To determine if ψNef contributes to the antagonism of rhesus tetherin, this sequence was cloned into an expression vector and tested for the ability to rescue the release of SIV Δ*nef* in the presence of rhesus tetherin. Whereas wild-type Nef rescued virus release as previously described (Jia et al., 2009), no increase in virus release was observed for ψNef (Figures S2B and S2C).

To determine if ψNef or EnvITM acquired other Nef functions that might contribute to the increased replicative capacity of SIV Δ*nefP*, ψNef and EnvITM were tested for MHC class I and CD4 downregulation, two functional activities that involve distinct Nef sequences and cellular mechanisms (Roeth and Collins, 2006). Neither ψNef nor EnvITM resulted in a detectable decrease in MHC class I expression (Figure S2D). Consistent with binding to CD4 as a receptor, wild-type Env and EnvITM both downregulated CD4 (Figure S2E). ψNef also resulted in a slight, but reproducible, decrease in the surface expression of CD4 (Figure S2E). However, since the extent of CD4 downregulation by ψNef was marginal compared to wild-type Nef (1.6-fold versus 6.1-fold), and was only detectable under conditions of protein overexpression, it is unclear to what extent this activity contributes to the replication of SIV Δ*nefP*.

To identify the specific amino acid changes in Env that confer resistance to rhesus tetherin, subsets of the ITM changes were introduced into SIV Δ*nef*, and these mutants were tested for resistance to increasing expression levels of rhesus tetherin. Five amino acid substitutions at the C-terminus of gp41 (IRATT) were sufficient for resistance to rhesus tetherin (Figures 4A, 4B and 4C). In contrast, neither the first six substitutions at the N-terminus (PIGPAH), nor three substitutions in the central region (IFE) of the gp41 tail, had a significant effect on virus release (Figures 4A, 4B and 4C). Subsets of the IRATT changes were also tested and found to have partial effects on resistance to rhesus tetherin (Figure S3). Thus, the ability of SIV Δ*nefP* to overcome restriction by rhesus tetherin depends on a combination of five residues at the C-terminus of gp41.

A conserved tyrosine-based endocytosis motif (GYXXΦ) in the membrane-proximal region of the gp41 tail was previously shown to be required for HIV-2 Env antagonism of tetherin (Abada et al., 2005; LeTortorec and Neil, 2009; Noble et al., 2006). We therefore asked whether this motif might also be important for EnvITM antagonism of rhesus tetherin. A tyrosine to alanine substitution was introduced at position 721 ($Y_{721}A$) of EnvITM in the context of SIV ITMΔ*nef*, and this mutant was tested for virus release in the presence of rhesus tetherin. This single amino acid substitution completely abrogated resistance to

rhesus tetherin (Figures 4D and 4E). Hence, SIV EnvITM and HIV-2 Env appear to use similar mechanisms to antagonize tetherin that depend on the membrane-proximal endocytosis motif in gp41.

Amino acid differences in the N-terminus of tetherin account for the resistance of SIV Δ*nefP* to rhesus tetherin, but not to human tetherin

Recombinants between human and rhesus tetherin were constructed to identify the residues responsible for the differential ability of these two proteins to restrict SIV Δ*nefP*. Sequences coding for the cytoplasmic domain (N) were exchanged to generate rN/hBST-2 and hN/rBST-2, and sequences coding for the transmembrane domain (TM) were exchanged to generate rTM/hBST-2 and hTM/rBST-2. These recombinants were then tested for the ability to inhibit virus release for SIV Δ*nefP*. SIV Δ*nefP* was restricted by hN/rBST-2 and rTM/hBST-2, but not by rN/hBST-2 or hTM/rBST-2 (Figures 5A and 5B). Thus, similar to wild-type SIV, the resistance of SIV Δ*nefP* is dependent on sequences in the cytoplasmic domain of rhesus tetherin.

To identify the cytoplasmic domain residues that account for the selective resistance of SIV Δ*nefP* to rhesus tetherin, amino acid substitutions were introduced at positions that differ from human tetherin (Figure 5C). Neither disruption of the D_{14}DIWK_{18} sequence in rhesus tetherin (rBST-2 AAAAA) nor the introduction of these residues into human tetherin (hBST-2 DDIWK) changed the pattern of restriction (Figure 5D). However, deletion of the first ten amino acids of rhesus tetherin (rBST-2 Δ10) resulted in the inhibition of virus release, indicating that these residues are essential for the ability of SIV Δ*nefP* to overcome restriction (Figure 5D). When residues 3–5 and 9–11 of rhesus tetherin were replaced with the corresponding residues of human tetherin (rBST-2 STS+CRV) SIV Δ*nefP* became susceptible to restriction. Conversely, the reciprocal amino acid replacements (hBST-2 PIL+RKM) alleviated restriction by human tetherin (Figure 5D). However, only partial effects were observed when residues 3–5 and 9–11 were exchanged separately (Figure 5D). Thus, the resistance of SIV Δ*nefP* is dependent on a combination of six residues at the N-terminus of rhesus tetherin, P_3IL+R_9KM, that differ from the corresponding residues of human tetherin. Perhaps not coincidentally, these sequences partially correspond to residues of human tetherin (S_3TS) recently identified as sites of Vpu-mediated ubiquitination (Tokarev et al. 2010).

EnvITM selectively co-immunoprecipites with rhesus tetherin

The ability of EnvITM to physically associate with rhesus tetherin was examined by co-immunoprecipitation. Tetherin was immunoprecipitated from lysates of 293T cells co-transfected with constructs expressing wild-type or mutant forms of human and rhesus tetherin, and either Env, EnvITM or EnvITM Y_{721}A. Immunoprecipitated proteins were separated by SDS-PAGE, and western blots were probed with monoclonal antibodies to SIV gp120 and to tetherin. EnvITM co-immunoprecipitated with rhesus tetherin, but not with human tetherin (Figure 6A). A weak association between wild-type Env and rhesus tetherin was also observed (Figure 6A). However, approximately 3.0- to 3.5-fold more EnvITM than wild-type Env immunoprecipitated with rhesus tetherin, as reflected by comparisons of the ratios of Env to BST-2 in immunoprecipitates (Env IP/BST-2 IP) or immunoprecipitated Env to total Env in whole cell lysates (Env IP/Env input) (Figure 6A). Thus, the ITM changes appear to stabilize a basal association between wild-type Env and rhesus tetherin.

To determine if residues 3–5 and 9–11 contribute to the specificity of this interaction, recombinants in which these sequences were exchanged between human and rhesus tetherin were tested for binding to EnvITM. Introduction of the P_3IL and R_9KM residues from rhesus tetherin into human tetherin (hPIL+RKM) resulted in a detectable interaction with

EnvITM (Figure 6A). Conversely, replacement of these sequences in rhesus tetherin with the corresponding residues of human tetherin (rSTS+CRV) dimished, but did not eliminate, this interaction (Figure 6A). These results are therefore consistent with the effects of amino acid changes at postions 3–5 and 9–11 on the susceptibility of SIV Δ*nefP* to restriction, and reveal a selective physical interaction between EnvITM and rhesus tetherin.

Since the P_3IL and R_9KM residues flank a conserved dual tyrosine-based endocytosis motif at positions 6–8 (Rollason et al., 2007), this motif was disrupted with alanine substitutions (rYDY/AAA) to determine if EnvITM binding was also dependent on these sequences. Although these mutations significantly impaired virus release for SIV Δ*nefP* (Figure 6B), they did not impair binding to EnvITM (Figure 6A). Likewise, the Y_{721}A mutation in EnvITM (EnvITM Y_{721}A), which abrogated virus release (Figures 4D and 4E), did not have a significant effect on binding to rhesus tetherin (Figure 6A). These results indicate that a physical interaction between EnvITM and rhesus tetherin is not sufficient for antagonism, and that these motifs may be required for interactions with cellular factors, possibly AP-2 complex proteins involved in clatharin-mediated endocytosis.

An alanine to aspartate substitution in the ectodomain of human tetherin (A_{100}D) was recently shown to disrupt antagonism by SIV_{agm}Tan and HIV-2 Env (Gupta et al., 2009; Lopez et al. 2010). We therefore introduced the corresponding mutation into rhesus tetherin (A_{103}D) to determine if this residue is also important for the interaction with EnvITM. This substitution did not impair binding to EnvITM (Figure 6A), or the release of SIV Δ*nefP* (Figure 6B). Therefore, unlike SIV_{agm}Tan or HIV-2 Env antagonism of human tetherin, this particular residue is not critical for the ability of EnvITM to oppose rhesus tetherin.

To determine if the cytoplasmic domain of EnvITM is sufficient to counteract rhesus tetherin, heterologous CD4-Env fusion proteins were tested for the ability to rescue particle release for an *env*- and *nef*-deleted strain of SIV. Constructs were engineered to express the ectodomain and transmembrane domain of CD4 fused to the cytoplasmic tail of Env or EnvITM (CD4-Env and CD4-ITM), or the ectodomain of CD4 fused to the transmembrane and cytoplasmic domains of Env or EnvITM (CD4-TM-Env and CD4-TM-ITM). Western blot analysis of transfected cell lysates revealed two bands for each of the CD4 fusion proteins, suggesting proteolytic degradation. Nevertheless, CD4-ITM, and to a lesser extent, CD4-TM-ITM, but not CD4-Env or CD4-TM-Env, restored particle release to similar levels as the complete EnvITM protein (Figure 6C).

The CD4-Env chimeras were then tested for a physical association with rhesus tetherin by co-immunoprecipitation. Consistent with the results obtained with the intact Env proteins, these interactions were stronger for the CD4 fusions containing the cytoplasmic tail of EnvITM (CD4-ITM and CD4-TM-ITM), than for those containing the cytoplasmic tail of Env (CD4-Env and CD4-TM-Env) (Figure 6D). Approximately 3.3- to 3.7-fold more CD4-ITM than CD4-Env, and 2.2- to 4.6-fold more CD4-TM-ITM than CD4-TM-Env, immunoprecipitated with rhesus tetherin (Figure 6D). The membrane-spanning domain of Env does not appear to contribute to this interaction, since inclusion of these sequences diminished the binding of CD4-TM-Env relative to CD4-Env and CD4-TM-ITM relative to CD4-ITM. Thus, the cytoplasmic domain of EnvITM is sufficient to stabilize a physical association with rhesus tetherin, and to overcome restriction by rhesus tetherin, when expressed as a heterologous CD4 fusion protein.

EnvITM downmodulates and co-localizes with rhesus tetherin in infected cells

We next asked whether SIV EnvITM could downmodulate tetherin from the surface of infected cells. Peripheral blood lymphocytes were infected with wild-type SIV, SIV Δ*nef*, SIV Δ*nefP* and SIV Δ*nefP* with the Y_{721}A mutation (SIV Δ*nefP* Y_{721}A). Five days post-

infection, the cultures were treated with IFNα, and stained 24 hours later for the surface expression of CD4 and tetherin, and for the intracellular expression of p27 capsid. The mean fluorescence intensity (MFI) of tetherin expression on the cell surface was compared for virus-infected ($p27^+$) $CD4^+$ lymphocytes. Consistent with a previous study showing Nef-mediated downregulation of rhesus tetherin in transfected cells (Jia et al., 2009), a 2.0-fold decrease in the surface expression of tetherin was observed for wild-type SIV versus SIV Δ*nef*-infected cells (Figure 7A). A decrease in the surface expression of tetherin was also observed in SIV Δ*nefP*-infected cells (Figure 7A). Although the extent of tetherin downregulation was less than in wild-type SIV-infected cells, this effect was completely eliminated by the $Y_{721}A$ mutation in SIV Δ*nefP* $Y_{721}A$-infected cells (Figure 7A). Thus, similar to HIV-2 Env (LeTortorec and Neil, 2009), the downmodulation of rhesus tetherin by SIV EnvITM depends on the tyrosine-based endocytosis motif in gp41.

To further investigate the fate of rhesus tetherin in SIV Δ*nefP*-infected cells, we examined the subcellular distribution of Env and tetherin in infected primary lymphocytes. In wild-type SIV-infected cells, there was little overlap in the distribution of Env and tetherin, and the intensity of tetherin staining was consistently lower than in SIV Δ*nef*-infected cells (Figures 7B and S4), perhaps reflecting a role for Nef in reducing the steady-state levels of tetherin. In SIV Δ*nef*-infected cells, Env and tetherin exhibited similar distributions and greater co-localization, either as a coincidence of their localization to the same subcellular compartments, or possibly as a result of a basal interaction between wild-type Env and rhesus tetherin. However, in the SIV Δ*nefP*-infected cells, the distribution of Env and tetherin was more focal, and patches of intense co-localization were observed at the plasma membrane and within intracellular compartments (Figures 7B and S4). These observations were corroborated by comparing the Pearson's correlation coefficients for the co-localization of Env and tetherin in images of twenty randomly selected cells infected with each virus. The extent of Env and tetherin co-localization was significantly higher for SIV Δ*nef*-versus wild-type SIV-infected cells ($p<0.001$) and for SIV Δ*nefP*-versus SIV Δ*nef*-infected cells ($p=0.003$) (Figure 7C). The greater co-localization of Env and tetherin in SIV Δ*nefP*-compared to SIV Δ*nef*-infected cells suggests that, similar to HIV-2 antagonism of human tetherin (LeTortorec and Neil, 2009), EnvITM associates with rhesus tetherin in infected cells, sequestering it from sites of virus budding at the plasma membrane.

DISCUSSION

Most natural SIV isolates, including viruses of the $SIV_{smm/mac}$, SIV_{agm} and SIV_{cpz} lineages, use Nef to counteract restriction by tetherin in their non-human primate hosts (Jia et al., 2009; Sauter et al., 2009; Zhang et al., 2009). Due to the absence of sequences in the cytoplasmic domain of human tetherin necessary for antagonism by Nef (Jia et al., 2009; Zhang et al., 2009), this function was assumed by the Vpu protein of HIV-1 (Neil et al., 2008; Van Damme et al., 2008), and the Env protein of HIV-2 (LeTortorec and Neil, 2009). Thus, at least three different lentiviral gene products have evolved to counteract tetherin. Yet, the significance of these countermeasures to lentiviral pathogenesis is not well understood. Here we show that compensatory changes in the cytoplasmic tail of gp41 restore resistance to tetherin in a *nef*-deleted strain of SIV that regained a pathogenic phenotype in rhesus macaques. These results are consistent with the adaptation of HIV-2 Env for antagonism of human tetherin, and suggest that the ability to overcome restriction by tetherin is important for lentiviral pathogenesis.

HIV-2 Env internalizes and sequesters tetherin within the *trans*-Golgi network, effectively removing it from sites of virus assembly at the plasma membrane, by a mechanism that depends on a conserved tyrosine-based endocytosis motif in the cytoplasmic domain of gp41 and a physical interaction with tetherin (LeTortorec and Neil, 2009). Antagonism of rhesus

tetherin by the Env protein of SIV Δ*nefP* (EnvITM) also requires the endocytosis motif in gp41, and the selective co-immunoprecipitation of EnvITM with rhesus tetherin suggests that a physical interaction, either direct or via a bridging factor, occurs between these two proteins. Moreover, tetherin was downmodulated from the cell surface and co-localized with Env to a greater extent in SIVΔ*nefP*-infected lymphocytes than in SIV Δ*nef*-infected lymphocytes. These results suggest that, similar to HIV-2 Env, EnvITM promotes the internalization and sequestration of rhesus tetherin away from sites of virus release.

However, unlike HIV-2 Env antagonism of human tetherin, which involves determinants in the extracellular domain of Env (Abada et al., 2005; LeTortorec and Neil, 2009), the cytoplasmic domain of EnvITM is sufficient to antagonize rhesus tetherin. Expression of the EnvITM tail as a CD4-Env fusion protein resulted in a physical interaction with rhesus tetherin and rescued virus release for SIV Δ*env*Δ*nef*. Furthermore, whereas the $A_{100}D$ mutation in the ectodomain of human tetherin abrogates antagonism by SIV_{agm}Tan and HIV-2 Env (Gupta et al., 2009; Lopez et al. 2010), the corresponding mutation in rhesus tetherin ($A_{103}D$) had no effect on the anti-tetherin activity of EnvITM. The specificity of EnvITM for rhesus tetherin is instead dependent on sequences in the cytoplasmic domain of rhesus tetherin (P_3IL+R_9KM) that differ from the sequences required for antagonism by Nef ($G/D_{14}DIWK_{18}$) (Jia et al., 2009; Zhang et al., 2009). This is supported by the concordance of EnvITM binding, and SIV Δ*nefP* resistance, to recombinant forms of tetherin in which residues 3–5 and 9–11 of rhesus and human tetherin were exchanged. Thus, in contrast to the mechanism by which HIV-2 and SIV_{agm}Tan Env antagonize human tetherin, EnvITM antagonism of rhesus tetherin is driven by specific determinants in the cytoplasmic domains of each of these molecules.

While the Env protein of SIV Δ*nefP* has clearly acquired the ability to antagonize rhesus tetherin, the effects of EnvITM versus Env on virus release were not commensurate with differences in tetherin binding and downregulation. The reasons for these disparities are unclear, but may be related to the difficulty of comparing static measurements of protein interactions and cell surface expression to the cumulative effects of an inherently dynamic process. If EnvITM-tetherin complexes form transiently during the process of antagonism, only a small fraction of the EnvITM protein in a cell may bind to rhesus tetherin at a given time. Furthermore, the biochemical conditions and multiple wash steps required to observe the association of these proteins by co-immunoprecipitation probably understimate the true extent of EnvITM-tetherin interactions in living cells. Disproportionate effects on virus release relative to tetherin downmodulation were also observed for HIV-2 Env (LeTortorec and Neil, 2009). As has been suggested for HIV-2 Env, EnvITM may neutralize the antiviral effects of tetherin without significant downmodulation, perhaps by redistributing the protein in the plasma membrane away from sites of virus budding prior to internalization. Paradoxically, this would reduce virus infectivity by decreasing the amount of Env available for the assembly of infectious virions, and might account for additional compensatory changes in SIV Δ*nefP*. The possibility that EnvITM may redistribute tetherin is consistent with the detection of significant amounts of EnvITM and tetherin on the surface of SIV Δ*nefP*-infected cells, and with previous studies showing that Vpu mutants that cannot internalize tetherin are able to partially counteract virus restriction (Miyagi et al., 2009; Schubert et al., 1996).

Relative to SIV Δ*nef*, SIV Δ*nefP* exhibits increased replicative capacity and pathogenicity in rhesus macaques. Five of six animals infected with SIV Δ*nefP* developed moderate viral loads that were detectable in plasma throughout the chronic phase of infection (Alexander et al., 2003). Set-point viral loads 24 weeks post-infection were approximately two logs higher in SIV Δ*nefP*-infected animals than in SIV Δ*nef*-infected animals (Alexander et al., 2003). The selective pressure to acquire specific substitutions in gp41 that confer resistance to

tetherin suggests that this activity is important for optimal virus replication *in vivo*. However, it should be noted that the ITM changes were not sufficient for pathogenesis when introduced into SIV Δ*nef* by themselves (Alexander et al., 2003). The U3 deletion may contribute to the replication of SIV Δ*nefP* by virture of reducing the size of the viral genome. Likewise, the ITM changes in gp41 result in a modest, but reproducible, two- to three-fold increase in the fusogenicity of Env, which may facilitate virus replication independently from their role in opposing tetherin (Alexander et al., 2003). ψNef may also enhance virus replication through subtle effects on the cell-surface expression of CD4 or by another mechanism that remains to be defined. Thus, perhaps not surprisingly, other compensatory changes, in addition to those that confer resistance to tetherin, are likely to play a role in the increased replicative capacity and pathogenicity of SIV Δ*nefP*.

The finding that the envelope glycoprotein of SIV can acquire the ability to antagonize tetherin in the absence of Nef is entirely consistent with the adaptation of HIV-2 Env for antagonism of human tetherin. These observations also support the hypothesis that adaptation to human tetherin may have contributed to the epidemic spread of HIV-1 and HIV-2 (Evans et al. 2010; Sauter et al., 2009). However, the use of Env to counteract tetherin may come at a cost to the efficiency of virus replication. In contrast to Nef or Vpu, which are small accessory proteins, Env is a large protein (879 amino acids in the case of $SIV_{mac}239$) that is essential for virus replication. Consequently, the need to devote a substantial fraction of the Env proteins produced by an infected cell to the antagonism of tetherin, rather than to the assembly of infectious virions, is likely to have a greater impact on viral fitness than the use of Nef or Vpu to overcome this restriction. Indeed, this may in part explain the lower level of virus replication, and the slower rate of disease progression, for individuals infected with HIV-2 versus HIV-1 (deSilva et al., 2008).

In summary, we have identified compensatory genetic changes that restore resistance to tetherin in a *nef*-deleted strain of SIV that reverted to a pathogenic phenotype after serial passage in rhesus macaques. Five amino acid substitutions in the cytoplasmic tail of gp41 were sufficient to provide resistance to rhesus tetherin, but not to human tetherin. These changes resulted in a selective physical interaction with rhesus tetherin and antagonism of rhesus tetherin by a mechanism similar to HIV-2 Env antagonism of human tetherin. Of the multitude of functional activities that have been attributed to Nef, the acquisition of anti-tetherin activity by Env in a *nef*-deleted strain of SIV that regained a pathogenic phenotype indicates that this function is particularly important for virus replication *in vivo*. Hence, these observations provide the most direct evidence to date that antagonism of tetherin is important for lentiviral pathogenesis.

EXPERIMENTAL PROCEDURES

Plasmid DNA constructs

Constructs for the expression of Env and Nef were based on pCGCG, and constructs for the expression of tetherin were based on pcDNA3 as previously described (Jia et al., 2009). Full-length proviral clones were assembled from p239SpSp5', pSP72-239-3', pSP72-239-3'Δ*nef* and p3'ITMΔ*nef*ΔUS138 (Alexander et al., 2003; Jia et al., 2009; Kestler et al., 1991; Regier and Desrosiers, 1990). See the Supplemental Experimental Procedures for additional details.

Virus replication assays in primary lymphocytes

Rhesus macaque PBMCs were CD8-depleted using anti-CD8 immunomagnetic beads (Invitrogen), activated with concanavalin A (5 μg/ml) (Sigma-Aldrich), and expanded in medium supplemented with IL-2 (20 U/ml) (NIH AIDS Research and Reference Reagent

Program). Activated lymphocytes (2×10^6 cells) were infected with wild-type SIV, SIV Δ*nef* and SIV Δ*nefP* (50 ng p27 eq.). Two days post-infection, the cultures were divided and maintained in medium with or without IFNα (100 U/ml) (Sigma). Virus replication was monitored by measuring the accumulation of SIV p27 in the cell culture supernatant by antigen-capture ELISA (Advanced Biosciences Laboratories).

Virus release assays

Virus release was measured by the accumulation of SIV p27 in the cell culture supernatant and expressed as the percentage of maximal release in the absence of tetherin according to previously described methods (Jia et al., 2009). See the Supplemental Experimental Procedures for details.

Western blots

Proteins were separated by electrophoresis on SDS-polyacrylamide gels, transferred to polyvinylidene fluoride (PVDF) membranes and detected on western blots by probing with antibodies to Env, p55/p27, BST-2, Nef, HA, CD4 and β-actin as previously described (Jia et al., 2009). Details are provided in the Supplemental Experimental Procedures.

Co-mmunoprecipitation assays

293T cells (6×10^5 cells) were co-transfected with constructs expressing wild-type and mutant forms of human or rhesus tetherin (2 μg) and either wild-type Env, EnvITM, EnvITM $Y_{721}A$ or CD4-Env fusion proteins (2 μg). Twenty-four hours later, cells were lysed with RIPA buffer (200 μl) and incubated on ice for 10 minutes. Insoluble cell debris was removed by centrifugation at 3,000 rpm. Precleared lysates were incubated on a rotating platform for 1 hour at 4°C with 1 μg of the anti-tetherin monoclonal antibody HM1.24, generously provided by Chugai Pharmaceutical Co. (Kanagawa, Japan). Protein A sepharose beads (50 μl) (GE Healthcare) were then added, and the incubation was continued overnight at 4°C. The beads were washed ten times in RIPA buffer (500 μl) and boiled in 2× SDS sample buffer. Proteins were separated by SDS-PAGE, and detected by probing western blots with the monoclonal antibodies KK42 (NIH AIDS Research and Reference Reagent Program) and HM1.24 to detect SIV Env and BST-2 respectively, and a polyclonal antibody to CD4 (Sigma-Aldrich) to detect the CD4-Env fusion proteins. See Supplemental Experimental Procedures for additional details on western blots. Band intensities were determined using ImageJ software (Rasband, W.S., Image, US. NIH, Bethesda, MD, http://rsb.info.nih.gov/ij, 1997–2008).

Confocal microscopy

Rhesus macaque PBMCs were activated with concanavalin A (5 μg/ml) and expanded in medium supplemented with IL-2 (20 U/ml). Activated lymphocytes (2×10^6 cells) were infected with wild-type SIV, SIV Δ*nef* and SIV Δ*nefP* (50 ng p27 eq.). Three days post-infection, the cells were treated with IFNα (1000 U/ml). Twenty-four hours later, the cells were washed and fixed for 5 minutes in 2% paraformaldehyde PBS. After three washes with PBS, the cells were resuspended in 100 mM glycine diluted in 10% normal goat serum in PBS with 0.2% fish skin gelatin, 0.1% Triton x100 and 0.02% sodium azide (10% NGS-PBS-FSG-Tx100-NaN_3) for 15 minutes. The cells were then washed three times in 10% NGS-PBS-FSG-Tx100-NaN_3, and stained. The monoclonal antibodies KK42 (IgG_1) and HM1.24 (IgG_{2a}) were used at a 1:250 and 1:500 dilutions to stain for Env and BST-2, respectively. The cells were subsequently stained with Alexa-488- and Alexa-568-conjugated goat anti-mouse secondary antibodies specific for IgG_{2a} and IgG_1 (Invitrogen) (1:1000), and with TO-PRO3 (Invitrogen) (1:5000) to visualize cell nuclei. After staining, the cells were washed and mounted on slides with antiquenching mounting-medium (Vector

Laboratories, Inc). Images were acquired using a Leica TCS SP5 II confocal microscope. ImageJ software was used to calculate the Pearson's correlation coefficients for the co-localization of Env and tetherin in images of 20 randomly selected cells (Zinchuk and Zinchuk, 2008). Differences in the correlation coefficients for cells infected with each virus were compared using an unpaired Student's *t*-test.

HIGHLIGHTS

- SIV gp41 changes acquired in the absence of Nef restore resistance to tetherin.
- Changes in the SIV gp41 tail are sufficient for antagonism of rhesus tetherin.
- Changes in the SIV gp41 tail stabilize a physical association with rhesus tetherin.
- Host-specific resistance maps to residues at the N-terminus of rhesus tetherin.

Supplementary Material

Refer to Web version on PubMed Central for supplementary material.

Acknowledgments

We thank Ronald Desrosiers (New England Primate Research Center) for providing p3'ITMΔnefΔUS138. We also thank Andrew Rahmberg and William Neidermyer, Jr. at the NEPRC for technical assistance. This work was supported by Public Health Service grants AI087498, AI071306, RR000168 and RR000164. DTE is an Elizabeth Glaser Scientist supported by the Elizabeth Glaser Pediatric AIDS Foundation.

REFERENCES

Abada P, Noble B, Cannon PM. Functional domains within the human immunodeficiency virus type 2 envelope protein required to enhance virus production. J Virol. 2005; 79:3627–3638. [PubMed: 15731257]

Alexander L, Illyinskii PO, Lang SM, Means RE, Lifson J, Mansfield K, Desrosiers RC. Determinants of increased replicative capacity of serially passaged simian immunodeficiency virus with nef deleted in rhesus monkeys. J Virol. 2003; 77:6823–6835. [PubMed: 12768002]

Baba TW, Jeong YS, Penninck D, Bronson R, Greene MF, Ruprecht RM. Pathogenicity of live, attenuated SIV after mucosal infection of neonatal macaques. Science. 1995; 267:1820–1824. [PubMed: 7892606]

Baba TW, Liska V, Khimani AH, Ray NB, Dailey PJ, Penninck D, Bronson R, Greene MF, McClure HM, Martin LN, et al. Live attenuated, multiply deleted simian immunodeficiency virus causes AIDS in infant and adult macaques. Nat Med. 1999; 5:194–203. [PubMed: 9930868]

Bour S, Schubert U, Peden K, Strebel K. The envelope glycoprotein of human immunodeficiency viru type 2 enhances viral particle release: a vpu-like factor? J Virol. 1996; 70:820–829. [PubMed: 8551620]

deSilva TI, Cotten M, Rowland-Jones SL. HIV-2: the forgotten AIDS virus. Trends Microbiol. 2008; 16:588–595. [PubMed: 18964021]

Evans DT, Serra-Moreno R, Singh RK, Guatelli JC. BST-2/tetherin: a new component of the innate immune response to enveloped viruses. Trends Microbiol. 2010; 18:388–396. [PubMed: 20688520]

Fitzpatrick K, Skasko M, Deerinck TJ, Crum J, Ellisman MH, Guatelli J. Direct restriction of virus release and incorporation of the interferon-induced protein BST-2 into HIV-1 particles. PLoS Pathog. 2010; 6:e1000701. [PubMed: 20221443]

Gottlinger HG. Virus kept on a leash. Nature. 2008; 451:406–408. [PubMed: 18200012]

Gupta RK, Mlcochova P, Pelchen-Matthews A, Petit SJ, Mattiuzzo G, Pillay D, Takeuchi Y, Marsh M, Towers G. Simian immunodeficiency virus envelope glycoprotein counteracts tetherin/BST2/

CD317 by intracellular sequestration. Proc Natl Acad Sci U S A. 2009; 106:20889–20894. [PubMed: 19864625]

Hammonds J, Wang J-J, Yi H, Spearman P. Immunoelectron microscopic evidence for tetherin/BST2 as a the physical bridge between HIV-1 virions and the plasma membrane. PLoS Pathog. 2010; 6:e1000749. [PubMed: 20140192]

Hauser H, Lopez LA, Yang SJ, Oldenburg JE, Exline CM, Guatelli JC, Cannon PM. HIV-1 Vpu and HIV-2 Env counteract BST-2/tetherin by sequestration in a perinuclear compartment. Retrovirology. 2010; 7:51. [PubMed: 20529266]

Jia B, Serra-Moreno R, Neidermyer W, Rahmberg A, Mackey J, Fofana IB, Johnson WE, Westmoreland S, Evans DT. Species-specific activity of SIV Nef and HIV-1 Vpu in overcoming restriction by tetherin/BST2. PLoS Pathog. 2009; 5:e1000429. [PubMed: 19436700]

Jouvenet N, Neil SJ, Zhadina M, Zang T, Kratovac Z, Lee Y, McNatt M, Hatziioannou T, Bieniasz PD. Broad-spectrum inhibition of retroviral and filoviral particle release by tetherin. J Virol. 2009; 83:1837–1844. [PubMed: 19036818]

Kaletsky RL, Francica JR, Agrawal-Gamse C, Bates P. Tetherin-mediated restriction of filovirus budding is antagonized by the Ebola glycoprotein. Proc Natl Acad Sci U S A. 2009; 106:2886–2891. [PubMed: 19179289]

Kestler HW, Ringler DJ, Mori K, Panicali DL, Sehgal PK, Daniel MD, Desrosiers RC. Importance of the nef gene for maintenance of high virus loads and for the development of AIDS. Cell. 1991; 65:651–662. [PubMed: 2032289]

Kupzig S, Korolchuk V, Rollason R, Sugden A, Wilde A, Banting G. Bst-2/HM1.24 is a raft-associated apical membrane protein with an unusual topology. Traffic. 2003; 4:694–709. [PubMed: 12956872]

LeTortorec A, Neil SJD. Antagonism and intracellular sequestration of human tetherin by the HIV-2 envelope glycoprotein. Journal of Virology. 2009; 83:11966–11978. [PubMed: 19740980]

Lopez LA, Yang SJ, Hauser H, Exline CM, Haworth KG, Oldenburg J, Cannon PM. Ebola virus glycoprotein counteracts BST-2/Tetherin restriction in a sequence-independent manner that does not require tetherin surface removal. J Virol. 2010; 84:7243–7255. [PubMed: 20444895]

Mansouri M, Viswanathan K, Douglas JL, Hines J, Gustin J, Moses AV, Fruh K. Molecular mechanism of BST2/tetherin downregulation by K5/MIR2 of Kaposi's sarcoma-associated herpesvirus. J Virol. 2009; 83:9672–9681. [PubMed: 19605472]

McNatt MW, Zang T, Hatziioannou T, Bartlett M, Fofana IB, Johnson WE, Neil SJ, Bieniasz PD. Species-specific activity of HIV-1 Vpu and positive selection of tetherin transmembrane domain variants. PLoS Pathog. 2009; 5:e1000300. [PubMed: 19214216]

Miyagi E, Andrew AJ, Kao S, Strebel K. Vpu enhances HIV-1 virus release in the absence of Bst-2 cell surface down-modulation and intracellular depletion. Proc Natl Acad Sci U S A. 2009; 106:2868–2873. [PubMed: 19196977]

Miyakawa K, Ryo A, Murakami T, Ohba K, Yamaoka S, Fukuda M, Guatelli J, Yamamoto N. BCA2/rabring7 promotes tetherin-dependent HIV-1 restriction. PLoS Pathog. 2009; 5:e1000700. [PubMed: 20019814]

Neil SJ, Zang T, Bieniasz PD. Tetherin inhibits retrovirus release and is antagonized by HIV-1 Vpu. Nature. 2008; 451:425–430. [PubMed: 18200009]

Noble B, Abada P, Nunez-Iglesias J, Cannon PM. Recruitment of the adaptor protein 2 complex by the human immunodeficiency virus type 2 envelope protein is necessary for high levels of virus release. J Virol. 2006; 80:2924–2932. [PubMed: 16501101]

Perez-Caballero D, Zang T, Ebrahimi A, McNatt MW, Gregory DA, Johnson MC, Bieniasz PD. Tetherin Inhibits HIV-1 Release by Directly Tethering Virions to Cells. Cell. 2009; 139:499–511. [PubMed: 19879838]

Regier DA, Desrosiers RC. The complete nucleotide sequence of a pathogenic molecular clone of simian immunodeficiency virus. AIDS Res Hum Retrovir. 1990; 6:1221–1231. [PubMed: 2078405]

Roeth JF, Collins KL. Human immunodeficiency virus type 1 Nef: adapting to intracellular trafficking pathways. Microbiol Mol Biol Rev. 2006; 70:548–563. [PubMed: 16760313]

Rollason R, Korolchuk V, Hamilton C, Schu P, Banting G. Clatharin-mediated endocytosis of a lipid-raft-associated protein is mediated through a dual tyrosine motif. J Cell Sci. 2007; 120:3850–3058. [PubMed: 17940069]

Sakuma T, Noda T, Urata S, Kawaoka Y, Yasuda J. Inhibition of Lassa and Marburg virus production by tetherin. J Virol. 2009; 83:2382–2385. [PubMed: 19091864]

Sauter D, Schindler M, Specht A, Landford WN, Munch J, Kim K-A, Votteler J, Schubert U, Bibollet-Ruche F, Keele BF, et al. Tetherin-driven adaptation of Vpu and Nef function and the evolution of pandemic and nonpandemic HIV-1 strains. Cell Host Microbe. 2009; 6:409–421. [PubMed: 19917496]

Schubert U, Bour S, Ferrer-Montiel AV, Montal M, Maldarell F, Strebel K. The two biological activities of human immunodeficiency virus type 1 Vpu protein involve two separable structural domains. J Virol. 1996; 70:809–819. [PubMed: 8551619]

Tokarev AA, Munguia J, Guatelli JC. Serine-threonine ubiquitination mediates downregulation of BST-2/tetherin and relief of restricted virion release by HIV-1 Vpu. J Virol. 2010 In press.

Van Damme N, Goff D, Katsura C, Jorgenson RL, Mitchell R, Johnson MC, Stephens EB, Guatelli J. The interferon-induced protein BST-2 restricts HIV-1 release and is downregulated from the cell surface by the viral Vpu protein. Cell Host Microbe. 2008; 3:245–252. [PubMed: 18342597]

Wolf D, Goff SP. Host restriction factors blocking retroviral replication. Annu Rev Genet. 2008; 42:143–163. [PubMed: 18624631]

Wyand MS, Manson KH, Lackner AA, Desrosiers RC. Resistance of neonatal monkeys to live attenuated vaccine strains of simian immunodeficiency virus. Nat Med. 1997; 3:32–36. [PubMed: 8986737]

Zhang F, Wilson SJ, Landford WC, Virgen B, Gregory D, Johnson MC, Munch J, Kirchhoff F, Bieniasz PD, Hatziioannou T. Nef proteins from simian immunodeficiency viruses are tetherin antagonists. Cell Host Microbe. 2009; 6:54–67. [PubMed: 19501037]

Zinchuk V, Zinchuk O. Quantitative colocalization analysis of confocal fluorescence microscopy images. Chapter 4. Curr Protoc Cell Biol. 2008 Unit 4 19.

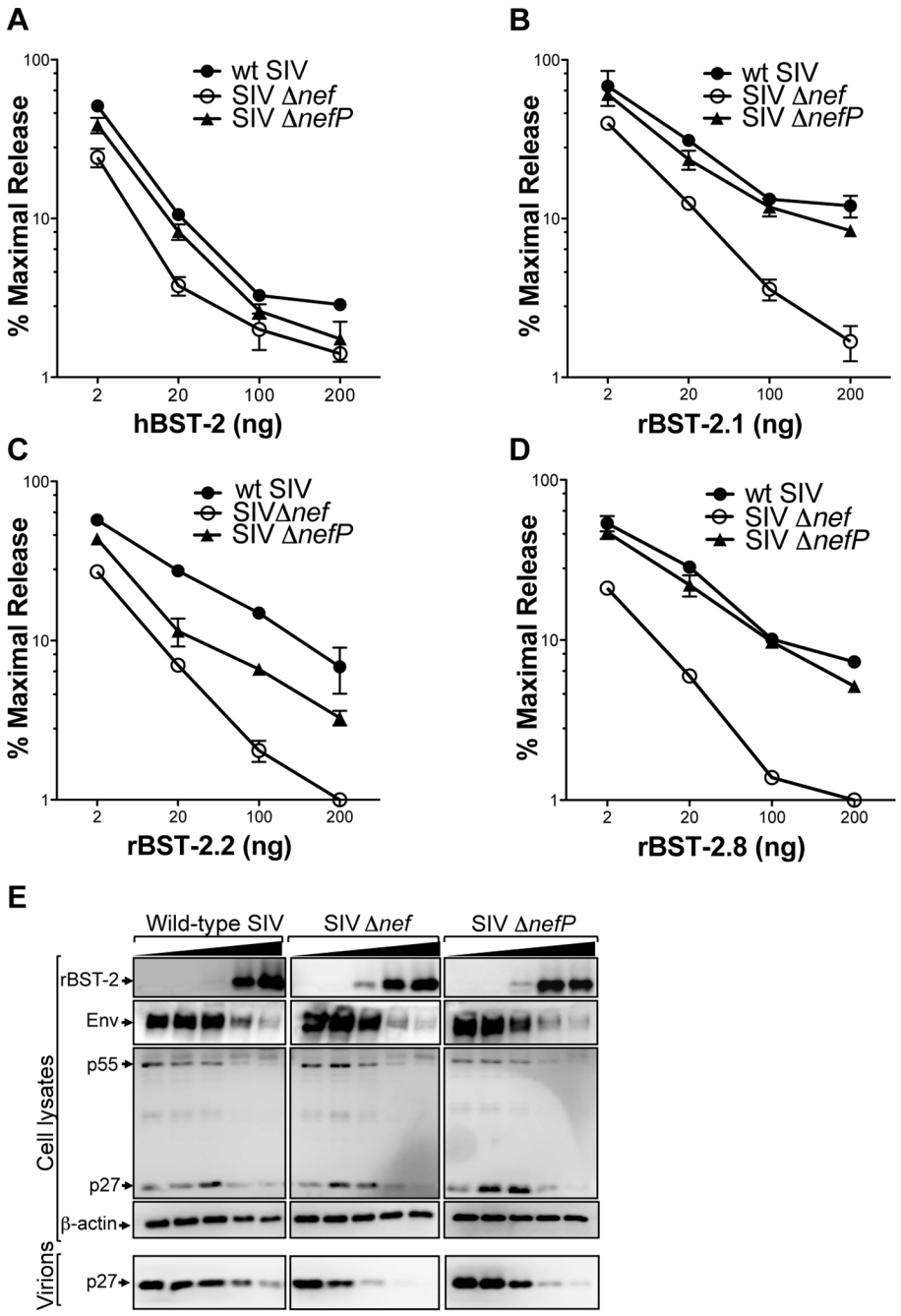

Figure 1. Compensatory genetic changes in SIV Δ*nefP* confer resistance to rhesus tetherin

Wild-type SIV, SIV Δ*nef* and SIV Δ*nefP* were tested for virus release in the presence of human tetherin (hBST-2), and three different alleles of rhesus tetherin (rBST-2.1, rBST-2.2 and rBST-2.8, see Figure S1). Virus release is shown at increasing amounts of plasmid DNA for hBST-2 (A), rBST-2.1 (B), rBST-2.2 (C), and rBST-2.8 (D). The amount of virus released into the cell culture supernatant was determined by SIV p27 antigen-capture ELISA 48 hours post-transfection from duplicate transfections, and the mean and standard deviation (+/− error bars) were calculated as a percentage of maximal virus release in the absence of tetherin. (E) The accumulation of virion-associated p27 in the cell culture supernatant was compared to Env and p55 Gag in cell lysates by western blot analysis.

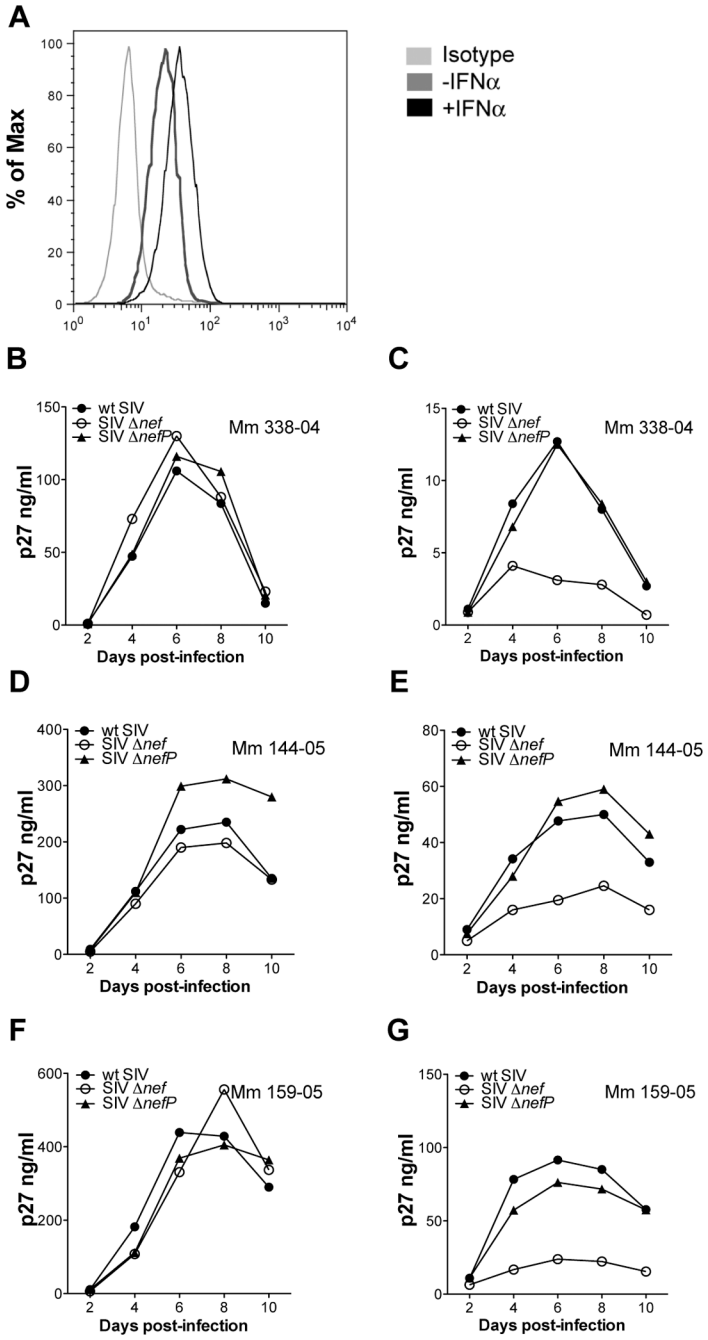

Figure 2. The compensatory changes in SIV Δ*nefP* enhance virus replication in interferon-treated rhesus macaque lymphocytes

Activated primary rhesus macaque lymphocytes were infected with wild-type SIV, SIV Δ*nef* and SIV Δ*nefP*. On day two post-infection, the cultures were divided and maintained in medium with or without IFNα. (A) The upregulation of tetherin on $CD4^+$ lymphocytes was verified by flow cytometry 24 hours after treatment with IFNα. Virus replication was monitored by the accumulation of p27 in the supernatant for cultures maintained without (B, D and F), or with (C, E and G), 100 U/ml IFNα.

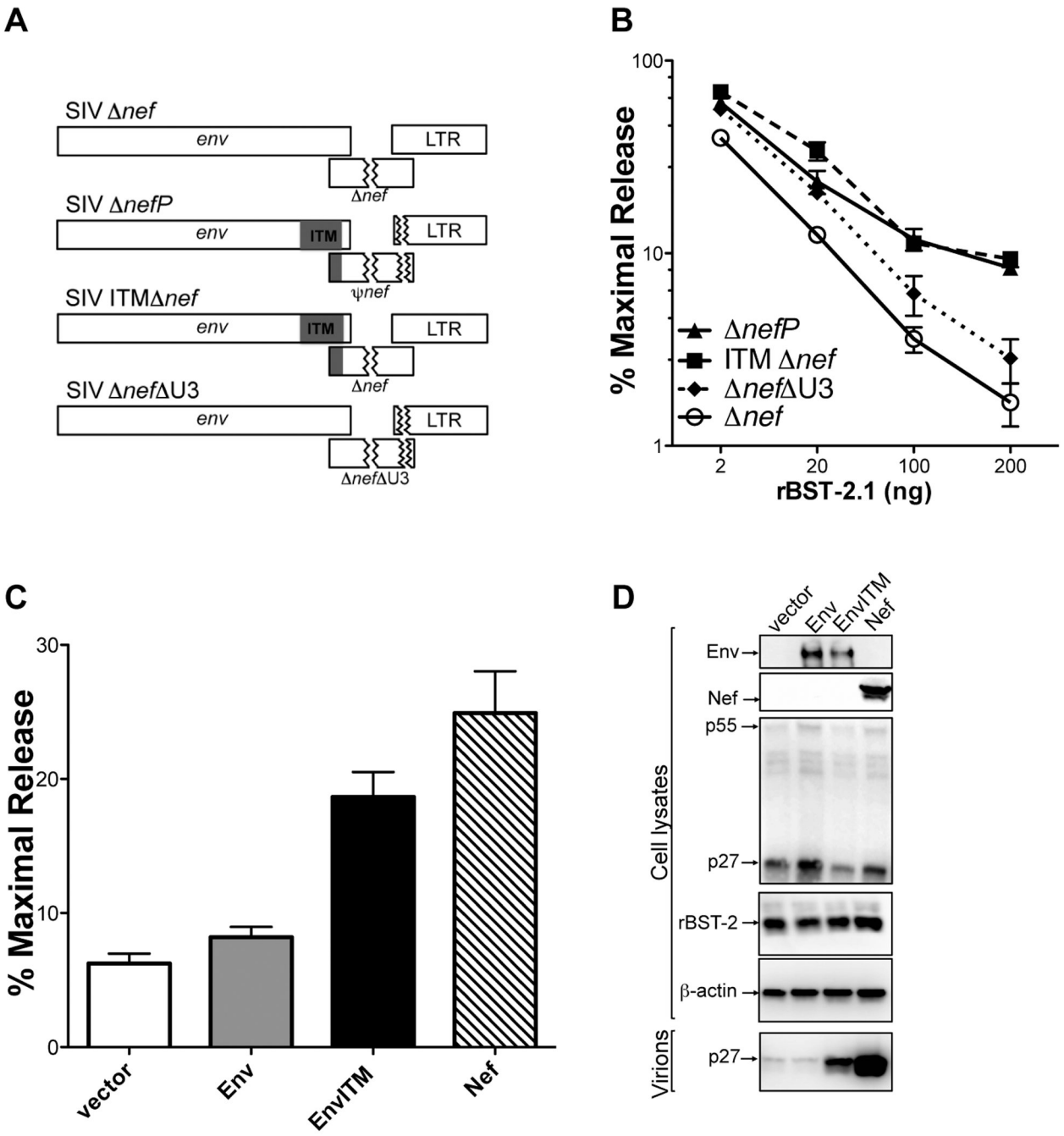

Figure 3. Amino acid substitutions in the cytoplasmic domain of gp41 account for the resistance of SIV Δ*nefP* to rhesus tetherin

(A) The ITM and ΔU3 changes were engineered separately into SIV Δ*nef*. (B) These recombinant proviruses were tested for virus release in the presence of increasing amounts of an expression construct for rhesus tetherin (rBST-2.1). (C and D) Wild-type Env, EnvITM and Nef were tested for the ability to rescue particle release for SIV Δ*env*Δ*nef* in the presence of rhesus tetherin. Virus release was measured by SIV p27 antigen-capture ELISA (C), and corroborated by comparing virion-associated p27 in cell culture supernatant to p55 Gag in cell lysates by western blot analysis (D). (B and C) Error bars represent the standard deviation (+/−) of mean percent maximal virus release.See also Figure S2.

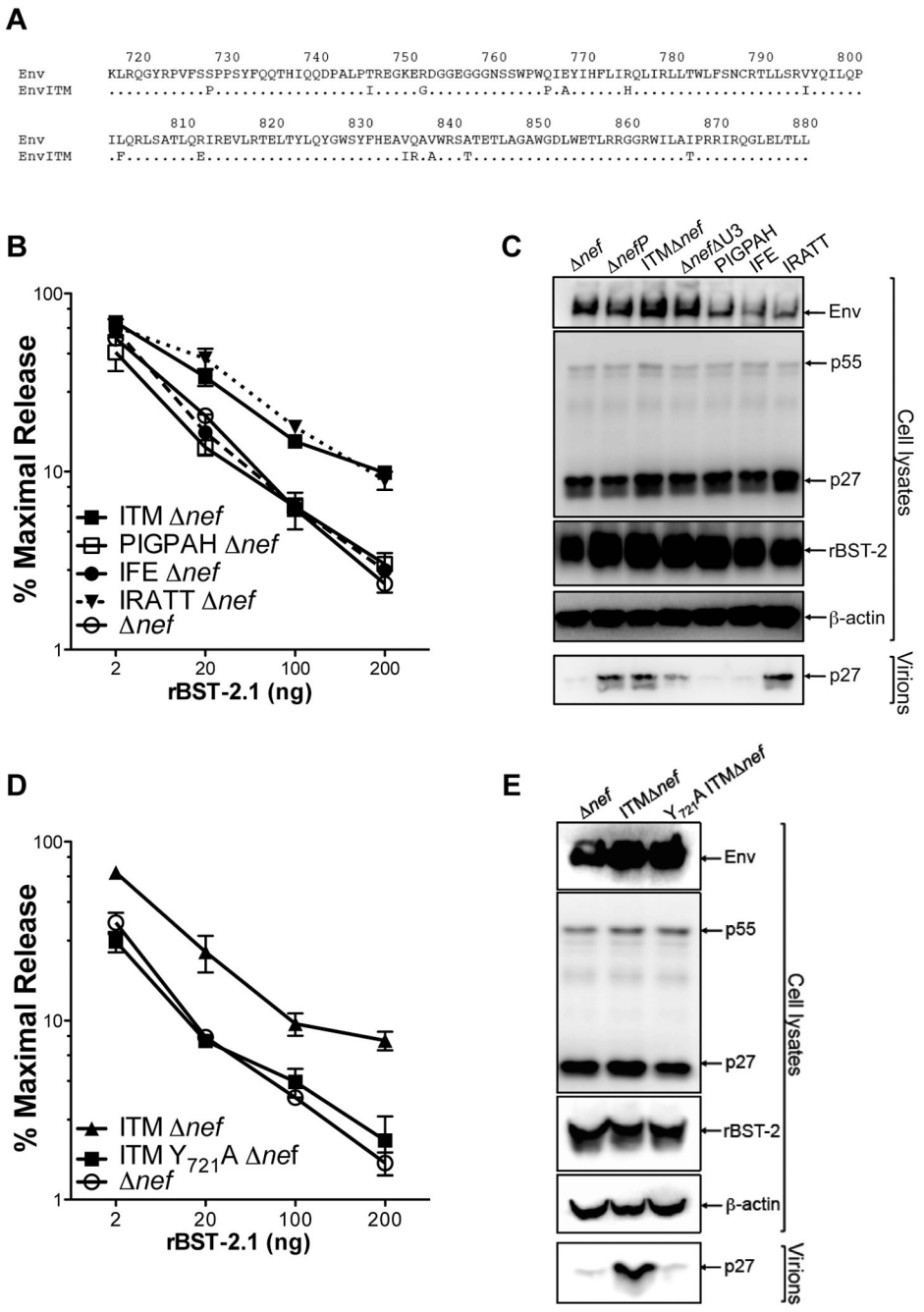

Figure 4. Identification of residues in the gp41 cytoplasmic domain required for the resistance of SIV Δ*nefP* to rhesus tetherin

(A) The gp41 cytoplasmic domains of SIV Δ*nefP* (EnvITM) and wild-type $SIV_{mac}239$ (Env) differ by 14 amino acids. (B and C) Subsets of the ITM changes were introduced into SIV Δ*nef* and tested for virus release in the presence of rhesus tetherin (rBST-2.1) by p27 antigen-capture ELISA (B) and by western blot analysis (C). These proviral constructs included six substitutions in the N-terminus (PIGPAH), three substitutions in the central region (IFE), and five substitutions in the C-terminus (IRATT) of the gp41 tail (see also Figure S3). (D and E) A tyrosine to alanine substitution was introduced at position 721 ($Y_{721}A$) in the context of SIV ITMΔ*nef*, and differences in the release of SIV Δ*nef*, SIV

ITMΔ*nef* and SIV Y_{721}A ITMΔ*nef* were compared by p27 antigen-capture ELISA (D) and by western blot analysis (E) in the presence of rhesus tetherin. (B and D) Error bars indicate the standard deviation (+/−) of mean percent maximal virus release.

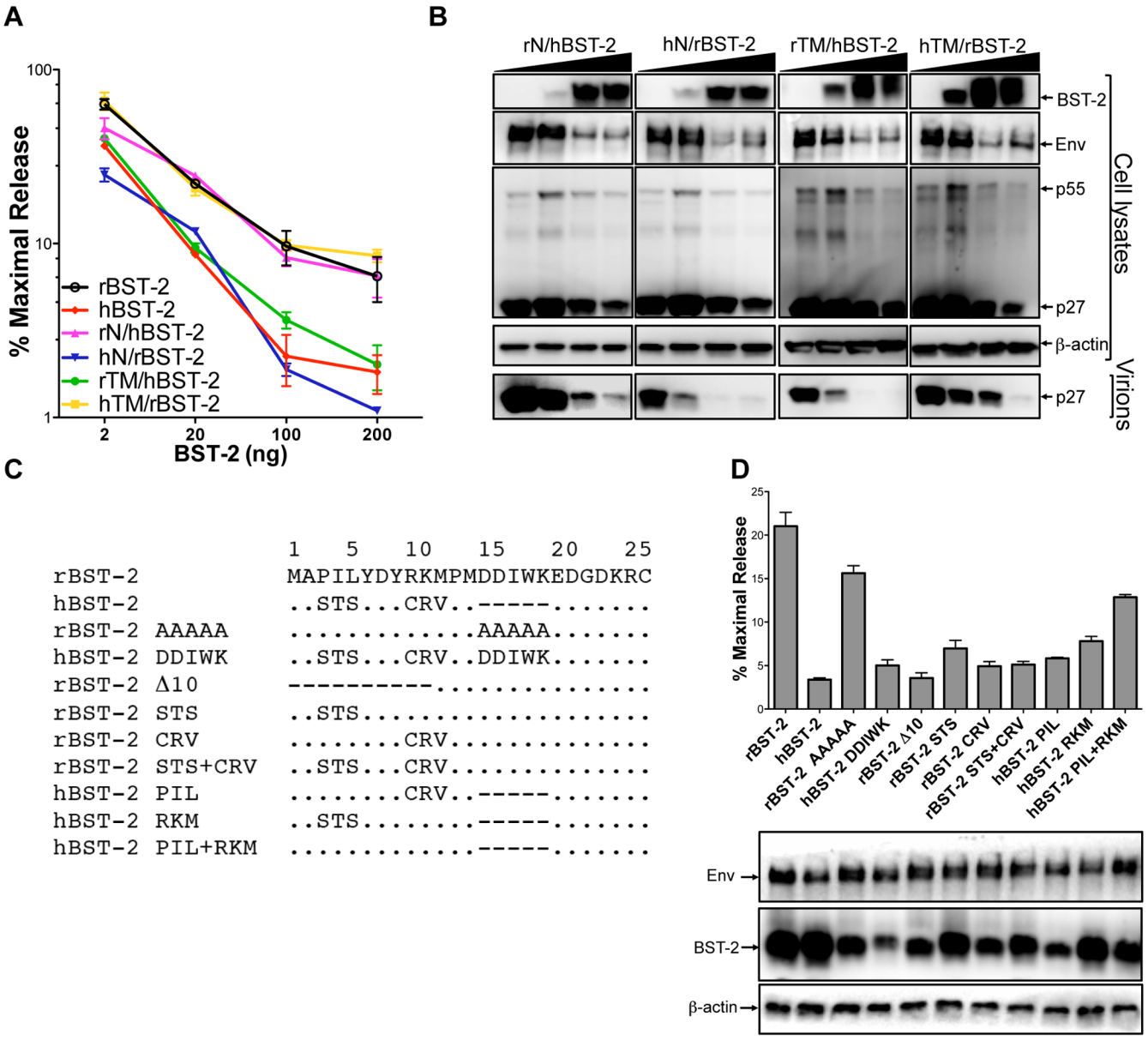

Figure 5. Identification of residues in the cytoplasmic domain of rhesus tetherin that confer susceptibility to SIV Δ*nefP*

Sequences coding for the cytoplasmic (N) and transmembrane (TM) domains of human and rhesus tetherin (rBST-2 and hBST-2) were exchanged to generate expression constructs for the following recombinants; rN/hBST-2, hN/rBST-2, rTM/hBST-2 and hTM/rBST-2. Virus release from 293T cells co-transfected with SIV Δ*nefP* proviral DNA and increasing amounts of each of the tetherin recombinants (2, 20, 100 and 200 ng) was determined by p27 antigen-capture ELISA (A) and verified by western blot analysis (B). (C) The indicated amino acid substitutions and deletions were introduced into the cytoplasmic domains of rhesus and human tetherin. (D) These mutants were tested for the ability to inhibit virus release for SIV Δ*nefP*. The expression of Env and each of the tetherin mutants was verified by western blot analysis of cell lysates. (A and D) Error bars indicate the standard deviation (+/−) of mean percent maximal virus release.

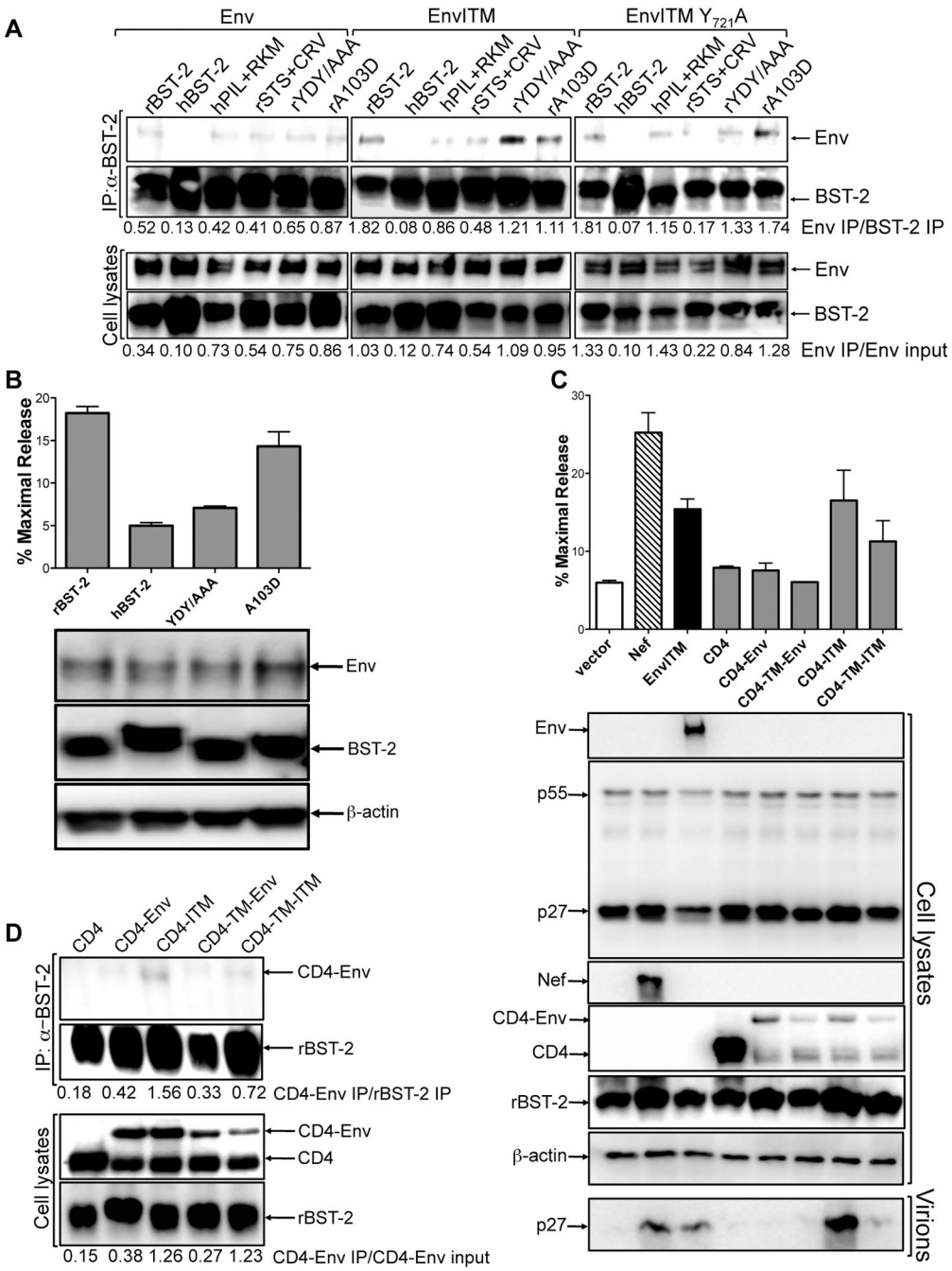

Figure 6. EnvITM selectively co-immunoprecipitates with rhesus tetherin

(A) Tetherin was immunoprecipitated from 293T cells co-transfected with constructs expressing wild-type or mutant forms of rhesus and human tetherin, and either Env, EnvITM or EnvITM $Y_{721}A$. Western blots were probed with monoclonal antibodies to Env and tetherin. The ratios of the relative band intensities for Env, EnvITM and EnvITM $Y_{721}A$ to BST-2 in immunoprecipitates (Env IP/BST-2 IP) and to total Env in whole cell lysates (Env IP/Env input) are indicated. The results shown are representative of three independent experiments. (B) Mutations in the dual tyrosine-based endocytosis motif (YDY/AAA) and position 103 in the ectodomain ($A_{103}D$) of rhesus tetherin were tested for their effects on the restriction of SIV Δ*nefP*, and the expression of Env and BST-2 was verified by western blot

analysis of cell lysates. (C) CD4 fusions with the cytoplasmic domains of Env and EnvITM (CD4-Env and CD4-ITM), and with the transmembrane and cytoplasmic domains of these proteins (CD4-TM-Env and CD4-TM-ITM), were tested for the ability to rescue particle release for SIV Δ*env*Δ*nef* in the presence of rhesus tetherin (rBST-2.1). Virus release was measured by p27 antigen-capture ELISA and verified by comparing virion-associated p27 in supernatant to p55 in cell lysates. Error bars represent the standard deviation of mean percent maximal virus release. (D) CD4-Env fusion proteins were tested for a physical interaction with rhesus tetherin. Tetherin was immunoprecipitated from 293T cells co-transfected with constructs expressing rBST-2.1, and either CD4, CD4-Env, CD4-ITM CD4-TM-Env or CD4-TM-ITM. Western blots were probed with antibodies to CD4 and BST-2. The ratios of the relative band intensities for each of the CD4-Env proteins to BST-2 inimmunoprecipitates (CD4-Env IP/BST-2 IP) and to total CD4-Env in whole cell lysates (CD4-Env IP/CD4-Env input) are indicated.

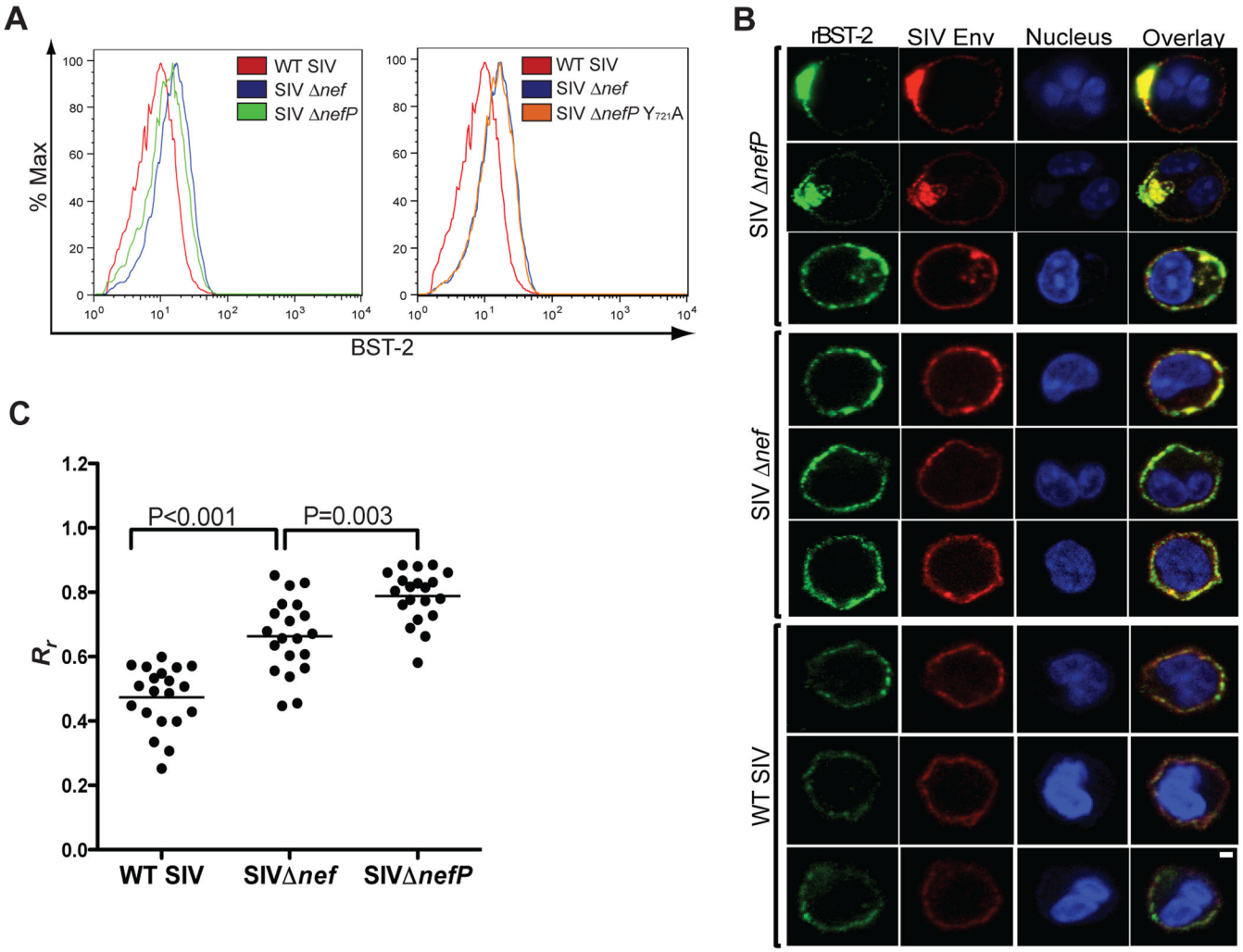

Figure 7. Tetherin is downmodulated from the cell surface and co-localizes with EnvITM in SIV Δ*nefP*-infected lymphocytes

(A) Activated primary rhesus macaque lymphocytes were infected with wild-type SIV, SIV Δ*nef*, SIV Δ*nefP* and SIV Δ*nefP* $Y_{721}A$. Five days post-infection, the cells were treated with IFNα, and stained 24 hours later for the surface expression of CD4 and tetherin (BST-2) and the intracellular expression of SIV p27. The MFI of BST-2 staining for lymphocytes infected with each virus is shown after gating on $p27^+$ $CD4^+$ cells. (B) Virus-infected lymphocytes were examined by confocal microscopy for the co-localization of Env and BST-2. Twenty-four hours after the addition of IFNα, the cells were fixed, permeabilized and stained with monoclonal antibodies to BST-2 (green), Env (red), and with a nuclear dye (blue). The scale bar corresponds to 1 μm. (C) The extent of Env and tetherin co-localization was estimated by calculating the Pearson's correlation coefficients for images of 20 randomly selected cells infected with each virus (see also Figure S4), and the differences in these values were compared for wild-type SIV- versus SIV Δ*nef*-infected cells and for SIV Δ*nef*- versus SIV Δ*nefP*-infected cells using an unpaired Student's *t*-test.